Supplementary Materials: Enhancement of the vegetation carbon uptake by the synergistic approach to air pollution control and carbon neutrality in China

Xiao Qin [1, 3], Guangming Shi [2, 3, *] and Fumo Yang [2, 3]

1. Model evaluation

The concentrations of meteorological and pollution fields simulated by the air quality model undergo multiple types of statistical parameters to verify the accuracy of the model simulation. mean fractional bias (MFB) and mean fractional error (MFE) represent the extent of fractional deviation from the mean and absolute error, respectively. Normalized mean bias (NMB) and normalized mean error (NME) indicate the average deviation and degree of deviation of the simulated values and observed values, respectively. To avoid over-discretization issues, these measures are standardized. Boylan et al [36] propose using MFB and MFE as indicators for assessing model simulation accuracy. The guidelines for the selection of ambient air quality models (trial) of China require employing methods such as NMB and NME to determine regional Eulerian grid model simulation accuracy.

Considering the aforementioned model evaluation indices, namely MFB, MFE, NMB, and NME, were employed as the evaluation metrics to validate the simulated meteorological parameters and pollutant concentrations by the WRF-Chem model using the subsequent equations.

$$MFB = \frac{2}{N} \sum_{i=1}^{N} \left(\frac{P_i - O_i}{P_i + O_i} \right)$$

$$MFE = \frac{2}{N} \sum_{I=1}^{N} \left(\frac{|P_i - O_i|}{P_i + O_i} \right)$$

$$NMB = \frac{\sum_{i=1}^{N}(P_i - O_i)}{\sum_{i=1}^{N} O_i} \times 100\%$$

$$NME = \frac{\sum_{i=1}^{N} |P_i - O_i|}{\sum_{i=1}^{N} O_i} \times 100\%$$

where Pi and Oi are modeled and observed variables; N is the number of valid samples involved in the comparison.

The meteorological fields simulated by the WRF model were validated using monitoring data from 439 meteorological stations across the country in this study. Specifically, the simulation results of the WRF model for January, April, July, and October 2016 were extracted and averaged with corresponding near-surface meteorological monitoring data obtained from the National Meteorological Science Data Centre (https://data.cma.cn/) for comparative analysis. Table S1 presents error statistics comparing the meteorological simulation results and observations.

According to the model evaluation method proposed by Boylan et al [36], if the MFB falls within the range of -60% to 60% and the MFE is less than 75%, the model simulation results are considered reasonably acceptable. Moreover, if MFB ranges from -30% to 30% and MFE is less than 50%, it indicates excellent model performance with desired simulation results. During our study period, when simulating China's meteorological field, both surface temperature and humidity exhibit MFB values between -30% and 30%, along with an MFE below 50%. These findings suggest that our model performs excellently, producing simulation results within desirable levels. Additionally, NMB and NME values are small while average deviations from observed surface values as well as average absolute errors remain minimal. In conclusion, our current model demonstrates superior simulation outcomes for the meteorological field in terms of accurately reflecting magnitudes and trends of surface meteorological parameters during this study period. It exhibits a certain level of representativeness and accuracy.

The simulation of the meteorological field in China during the study period demonstrates excellent model performance, with surface temperature and humidity MFB values ranging between -30% and 30%, and an MFE below 50%. These results indicate that the simulation outcomes are within the desired range, while NMB and NME values remain small. Moreover, both the average deviation of surface simulation results from observed values and the average absolute error are minimal. Consequently, this model exhibits superior accuracy in simulating meteorological parameters at the surface level during the study period, providing representative and precise insights.

To evaluate the validity of model simulations, we compared the monthly mean values of O_3 and $PM_{2.5}$ concentrations simulated by WRF-Chem with hourly-resolved automated data obtained from 1425 state-controlled monitoring stations across China during the study period. During our simulation period (Table S2), we observed that both ozone (O_3) and fine particulate matter ($PM_{2.5}$) concentrations exhibited moderate deviations, with MFB ranging from -60% to 60%. Additionally, MFE remained below 75%, suggesting a reasonable agreement between modeled and observed values for these pollutants. Specifically for July, our analysis reveals exceptional performance in modeling ozone concentration as indicated by MFBs within a range of -30% to 30% alongside MFEs lower than 50%. The positive NMB values indicate a slight overestimation of O_3 and $PM_{2.5}$ concentrations in most regions of China by the model, with NMB values below 30% in all months except April, suggesting a small average deviation from observed values in the simulation results. Thus, the WRF-Chem simulation of regional O_3 and $PM_{2.5}$ in China can effectively reflect actual observations. However, further improvement of the simulation results necessitates more comprehensive discussions on optimizing pollutant emission inventory and selecting appropriate physicochemical parameterization schemes.

The positive NMB values indicate a slight overestimation of O_3 and $PM_{2.5}$ concentrations in most regions of China by the model, with NMB values below 30% in all months except April, suggesting a small average deviation from observed values in the simulation results. Thus, the WRF-Chem simulation of regional O_3 and $PM_{2.5}$ in China can effectively reflect actual observations. However, further improvement of the simulation results necessitates more comprehensive discussions on optimizing pollutant emission inventory and selecting appropriate physicochemical parameterization schemes.

To validate the simulated GPP, we employed the gridded benchmark product MYD17A2H for the year 2016, which is derived from the MODIS-PSN algorithm [42]. This dataset was processed using Google Earth Engine (GEE) [65] to export monthly scales and interpolated to match the spatial resolution of the simulated GPP. The simulated GPP effectively replicated the observed spatial patterns with strong correlation coefficients (R=0.57-0.77, P<0.001) and exhibited relatively low model-observation bias (nationwide RMSE<67.10 gC/m²) (Table S6).

2. Tables

Table S1. Error statistics of meteorological simulation results and observations.

Meteorological element	Time	MFB(%)	MFE(%)	NMB(%)	NME(%)
Surface humidity	January	1.80	14.45	3.36	13.47
	April	6.20	18.65	7.02	17.62
	July	-4.61	9.69	-4.72	9.89
	October	-2.92	7.21	-2.53	7.00
Surface temperature	January	26.31	34.42	-23.15	38.75
	April	-1.16	13.59	-3.69	11.32
	July	2.77	8.59	1.35	7.51
	October	5.73	15.20	2.84	12.08

Table S2. Error statistics for the simulation results of $PM_{2.5}$ and O_3 concentrations.

Pollutants	Month	MFB (%)	MFE (%)	NMB (%)	NME (%)
$PM_{2.5}$	January	18.37	62.83	12.91	55.58
	April	43.76	57.93	35.63	46.90
	July	32.94	61.66	23.59	50.53
	October	17.99	54.87	10.43	49.52
O_3	January	36.19	68.45	23.22	58.46
	April	49.48	61.65	38.71	47.63
	July	0.78	32.16	0.47	30.93
	October	33.61	56.17	23.42	46.36

Table S3. Impact of PER, global climate change, and the coupled effect of these two factors on GPP in China.

Month	BL (TgC)	CN-BL (TgC)	CC-BL (TgC)				CE-BL (TgC)			
			SSP126	SSP245	SSP370	SSP585	SSP126	SSP245	SSP370	SSP585
January	146.98	13.81 (9.40%)	-52.78 (-35.91%)	-4.65 (-3.16%)	-13.80 (-9.39%)	2.94 (2.00%)	-43.53 (-29.62%)	5.14 (3.50%)	-1.51 (-1.03%)	16.01 (10.89%)
April	581.70	14.21 (2.44%)	-3.49 (-0.60%)	36.91 (6.35%)	-17.24 (-2.96%)	36.98 (6.36%)	9.40 (1.62%)	52.74 (9.07%)	-3.84 (-0.66%)	53.64 (9.22%)
July	1155.07	20.96 (1.81%)	-21.24 (-1.84%)	-28.94 (-2.51%)	-26.37 (-2.28%)	-53.31 (-4.62%)	-2.88 (-0.25%)	-8.19 (-0.71%)	-5.68 (-0.49%)	-28.92 (-2.50%)
October	503.23	19.65 (3.90%)	37.82 (7.52%)	-48.01 (-9.54%)	40.25 (8.00%)	15.95 (3.17%)	58.85 (11.69%)	19.65 (3.90%)	66.99 (13.31%)	38.29 (7.61%)
Total	2386.98	68.63 (2.88%)	-39.69 (-1.66%)	-44.69 (-1.87%)	-17.16 (-0.72%)	2.56 (0.11%)	21.84 (0.91%)	69.34 (2.90%)	55.96 (2.34%)	79.04 (3.31%)

Table S4. Coupled effects of carbon-neutral pollutant emission reduction policies and global climate change on provincial GPP in China.

Province	SSP126	SSP245	SSP370	SSP585	January	April	July	October
Hebei	-7.6	-7.37	-0.72	-8.21	-1.06	-2.51	-30.14	7
Shanxi	-5.08	-0.08	1.88	-0.97	-1.3	4.15	-13.4	7.23
Jilin	-0.51	-2.62	-4.98	-3.22	0	-1.8	-15.51	10.03
Liaoning	-2.06	-4.36	4.06	-2.73	-0.04	-1.71	-19.16	7.71
Heilongjiang	9.26	10.3	17.17	-1.89	0	22.57	-19.94	23.15
Shaanxi	-3.14	1.09	17.29	1.36	-7.13	5.82	-1.94	11.62
Gansu	-1.61	3.15	26.43	4.42	-1.17	3.5	3.21	8.65
Qinhai	1.03	10.95	16.75	10.94	0.01	5.1	40.18	-4.17
Shandong	-3.4	-6.93	-2.15	-8.27	-2.06	0.65	-25.16	6.52
Fujian	0.57	4.58	4.02	-1.56	-2.31	7.61	-2.48	0.07
Zhejiang	5.52	4.07	3.13	0.08	-4.08	10.22	4.24	4.01
Taiwan	0.1	0.94	1.12	0.72	-1.74	1.97	-1.02	0.96
Henan	-5.27	-5.65	6.23	-4.57	-7.61	13.62	-25.94	7.15
Hubei	1.08	-4.43	3.31	1.4	-7.84	12	-11.11	8.52
Hunan	4.49	1.98	7.36	3.14	-3.69	17.74	-3.79	-0.86
Jiangxi	8.89	9.28	7.88	3.98	-0.83	18.72	6.52	5.31
Jiangsu	2.78	-0.5	3.58	2.67	-2.5	6.15	-2.72	4.33
Anhui	2.86	-1.18	-2.71	1.92	-6.09	8.76	-2.61	6.81
Guangdong	-4.14	3.78	-8.6	-2.97	5.32	1.88	-11	-5.51
Hainan	-2.74	-2.27	10.08	-2.17	-1.31	-6.28	-0.74	-1.47
Sichuan	3.32	6.6	15.29	14.97	-5.71	1.84	17.08	24.38
Guizhou	8.51	10.41	-22.69	13.36	0.16	5.98	15.37	13.36
Yunnan	-13.13	1.68	-25.65	16.36	26.73	-58.35	-0.21	11.46
Beijing	-0.63	-0.7	-0.39	-0.97	-0.04	-0.77	-2.28	0.42
Shanghai	0.03	0	-0.17	0.03	-0.03	0.06	-0.04	0.05
Tianjing	-0.42	-0.46	0.66	-0.59	-0.02	-0.28	-1.68	0.36
Chongqing	2.25	-1.07	-3.13	1.93	-3.4	4.13	-3.65	6.84
Inner Mongolia	7.55	1.43	0.82	7.26	-0.03	16.01	-31.65	27.97
Xinjiang	7.59	7.75	6.44	8.98	-1.12	8.14	13.92	8.14
Ningxia	-0.14	1.02	-6.19	1.44	-0.03	1.12	1.2	1.71
Guangxi	-4.6	5.41	15.73	3.08	2.89	3.42	3.04	-13.33
Tibet	10.51	22.62	23.6	19.1	2.22	2.48	75.74	-4.61

Hong Kong	0	0	0	0	0	0	0	0
Macao	0	0	0	0	0	0	0	0

Table S5. Information of the other three CMIP6 models.

CMIP6 Model	Spatial Resolution	Synopsis
CanESM5	Land: 2.80×2.80 degree Ocean: 1.00×1.00 degree	Global climate models developed by the Canadian Meteorological Centre (CMC)
INM-CM4-8	Land: 2.00×1.50 degree Ocean: 0.50×0.50 degree	Climate model developed by the Institute of Mathematics of the Russian Academy of Sciences (INM)
INM-CM5-0	Land: 2.00×1.50 degree Ocean: 0.50×0.25 degree	A climate model developed by the Institute of Mathematics (INM) of the Russian Academy of Sciences, which was released in 2016

Table S6. Comparison of simulated GPP and benchmark values of each model in 2016.

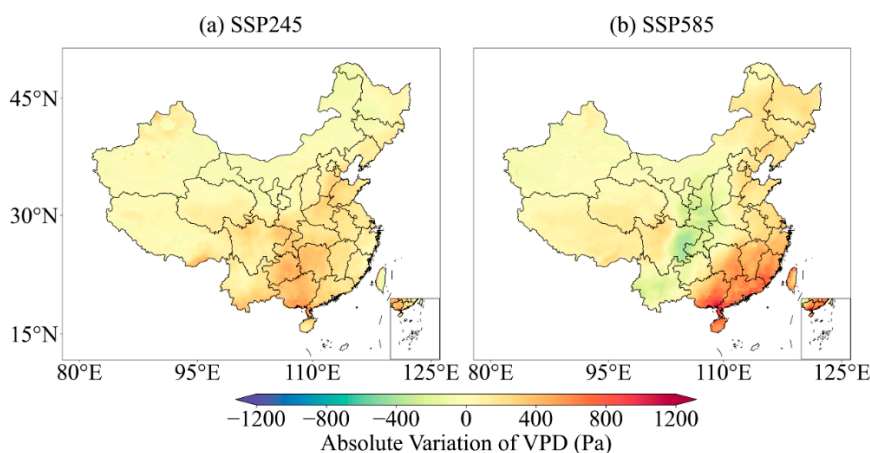| Model	Month	Pearson Correlation Coefficient	RMSE (gC/m^2)
MPI-ESM1-2-HR	January	0.76	22.85
	April	0.77	59.53
	July	0.57	67.10
	October	0.77	54.04
CanESM5	January	0.77	53.89
	April	0.71	82.14
	July	0.58	71.91
	October	0.76	90.44
INM-CM4-8	January	0.72	70.18
	April	0.71	106.40
	July	0.45	94.03
	October	0.72	96.54
INM-CM5-0	January	0.74	67.87
	April	0.70	102.55
	July	0.42	92.89
	October	0.72	93.08

3. Figures

Figure S1. Impact of global climate change on the spatio-temporal distribution of VPD in October under (a) the SSP245 scenario and (b) SSP585 scenario.
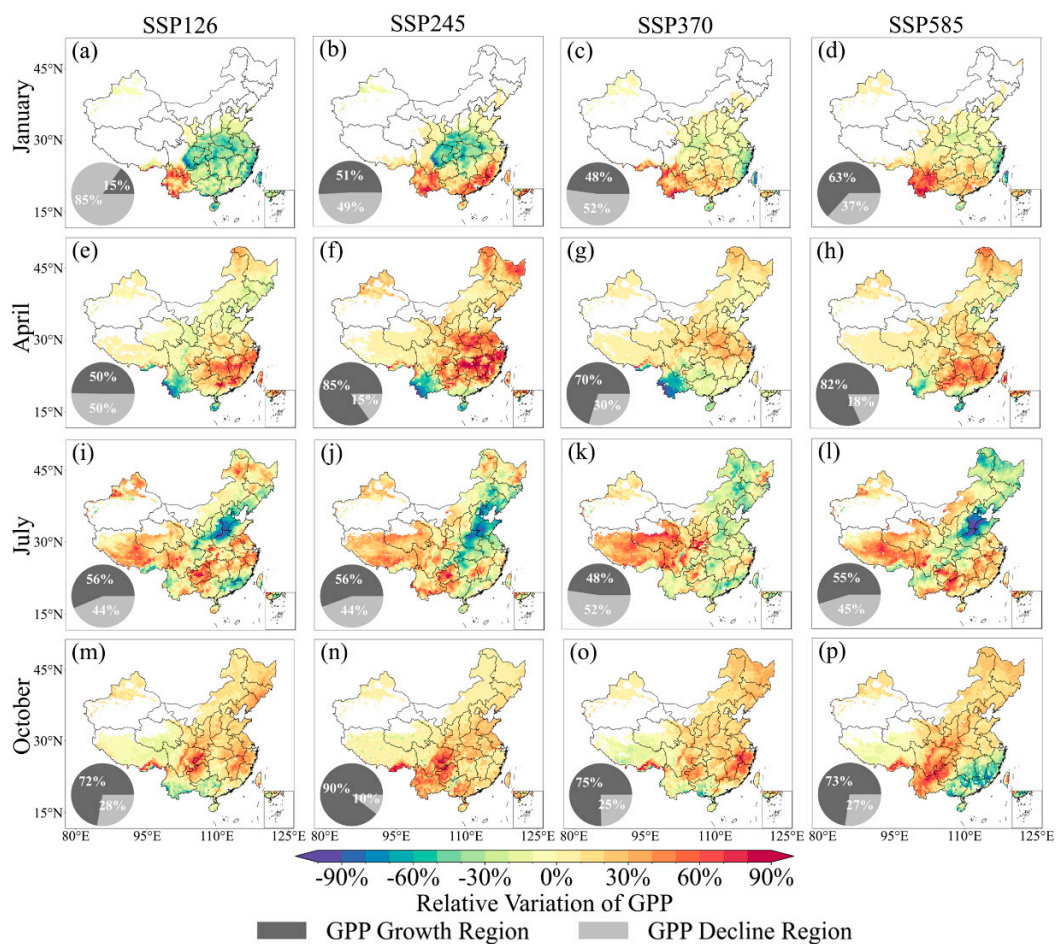

Figure S2. Coupled effects of carbon-neutral pollutant emission reduction policies and global climate change on GPP in January under the (a) SSP126, (b) SSP245, (c) SSP370, and (d) SSP585 scenarios; in April under the (e) SSP126, (f) SSP245, (g) SSP370, and (h) SSP585 scenarios; in July under the (i) SSP126, (j) SSP245, (k) SSP370, and (l) SSP585 scenarios; in October under the (m) SSP126, (n) SSP245, (o) SSP370, and (m) SSP585 scenarios. Pie charts represent the proportion of regions with increasing and decreasing GPP.
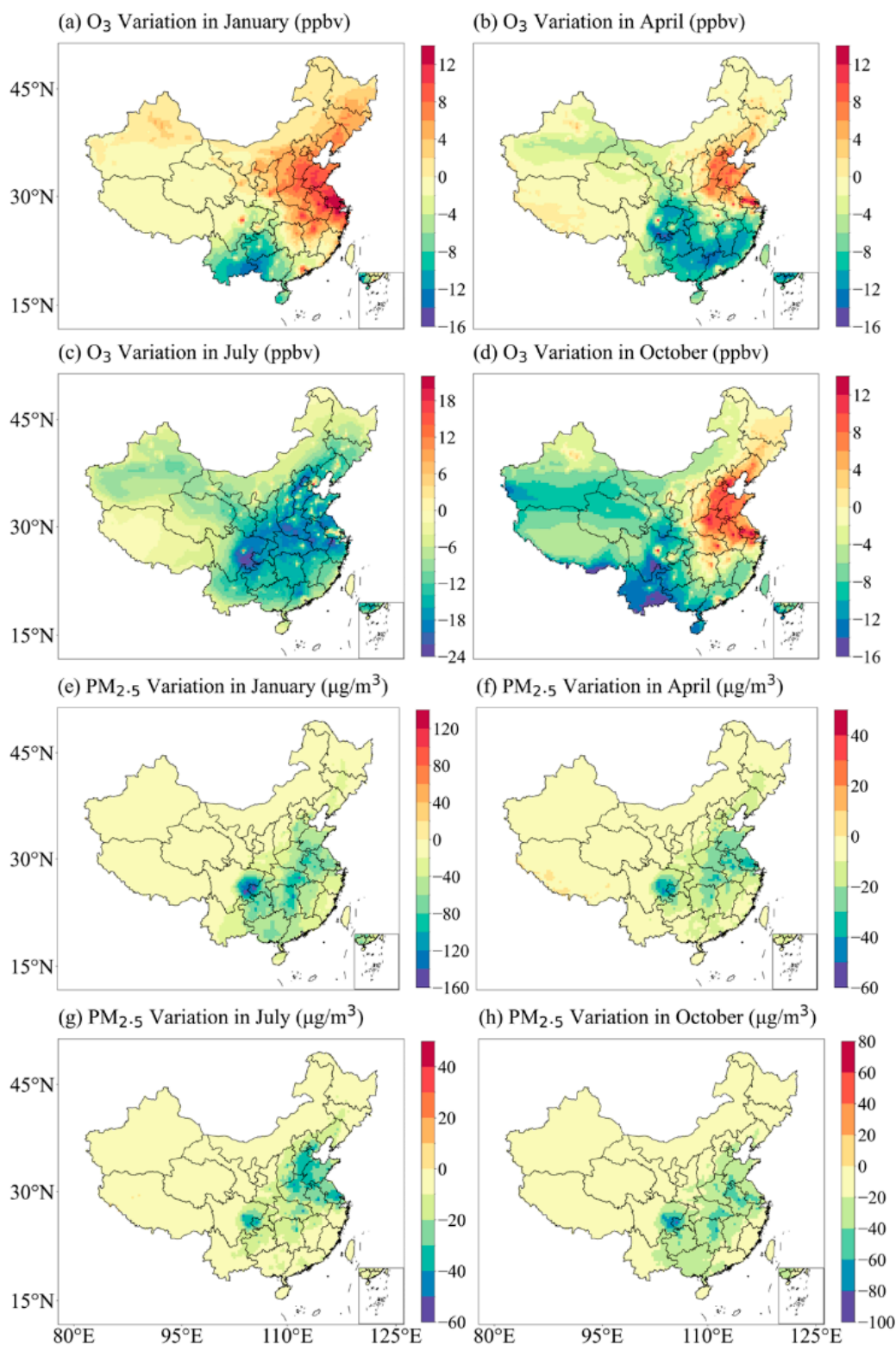
Figure S3. Impacts of carbon-neutral pollutant emission reduction policies on O₃ concentrations in (a) January, (b) April, (c) April, and (d) October and PM₂.₅ concentrations in (e) January, (f) April, (g) April, and (h) October in China.